

Determination of radar chaff diameter distribution function, fall speed, and concentration in the atmosphere by use of the NEXRAD radar

W. Patrick Arnott, Arlen Huggins, Jack Gilles, David Kingsmill, and John Walker

Desert Research Institute

Reno, NV 89512

ABSTRACT

Military aircraft use thin wires (i.e. radar chaff) to confuse enemy radar, and is usually formed by coating an SiO₂ core with aluminum. Chaff density was found to vary with chaff diameter, as the aluminum coating was not uniform. An optical diffraction technique was employed to obtain the distribution of chaff diameters. A normal distribution function provided an excellent fit to the measured diameter distribution. Chaff mass was measured, and the number of chaff per delivery tube was estimated to be 5.1 million. Chaff fall speed was investigated both in theory and measurement using a 25' fall tower. An estimate of chaff concentration in a cloud-free atmosphere from NEXRAD radar is described. Chaff concentration estimates from radar provide a possible means of estimating surface exposure of chaff, for estimation of health and ecosystem influence. Chaff is also useful in providing a meteorological tracer in atmospheric dynamics. A theoretical expression is given for determination of chaff concentration from the NEXRAD radar.

Table of Contents

DETERMINATION OF RADAR CHAFF DIAMETER DISTRIBUTION FUNCTION, FALL SPEED, AND CONCENTRATION IN THE ATMOSPHERE BY USE OF THE NEXRAD RADAR	1
ABSTRACT.....	1
INTRODUCTION	3
MEASUREMENT OF CHAFF DIAMETER DISTRIBUTION BY LASER DIFFRACTION	3
CHAFF MASS AND DENSITY	6
CHAFF FALL SPEED.....	8
FALL SPEED THEORY	8
CHAFF FALL SPEED MEASUREMENTS.....	13
TABLE 3	17
CHAFF RADAR CROSS SECTION.....	18
CHAFF RADAR CROSS SECTION FOR INHOMOGENEOUS CHAFF DELIVERY TUBES.....	21
TABLE 4.....	25
REFERENCES	28

Introduction

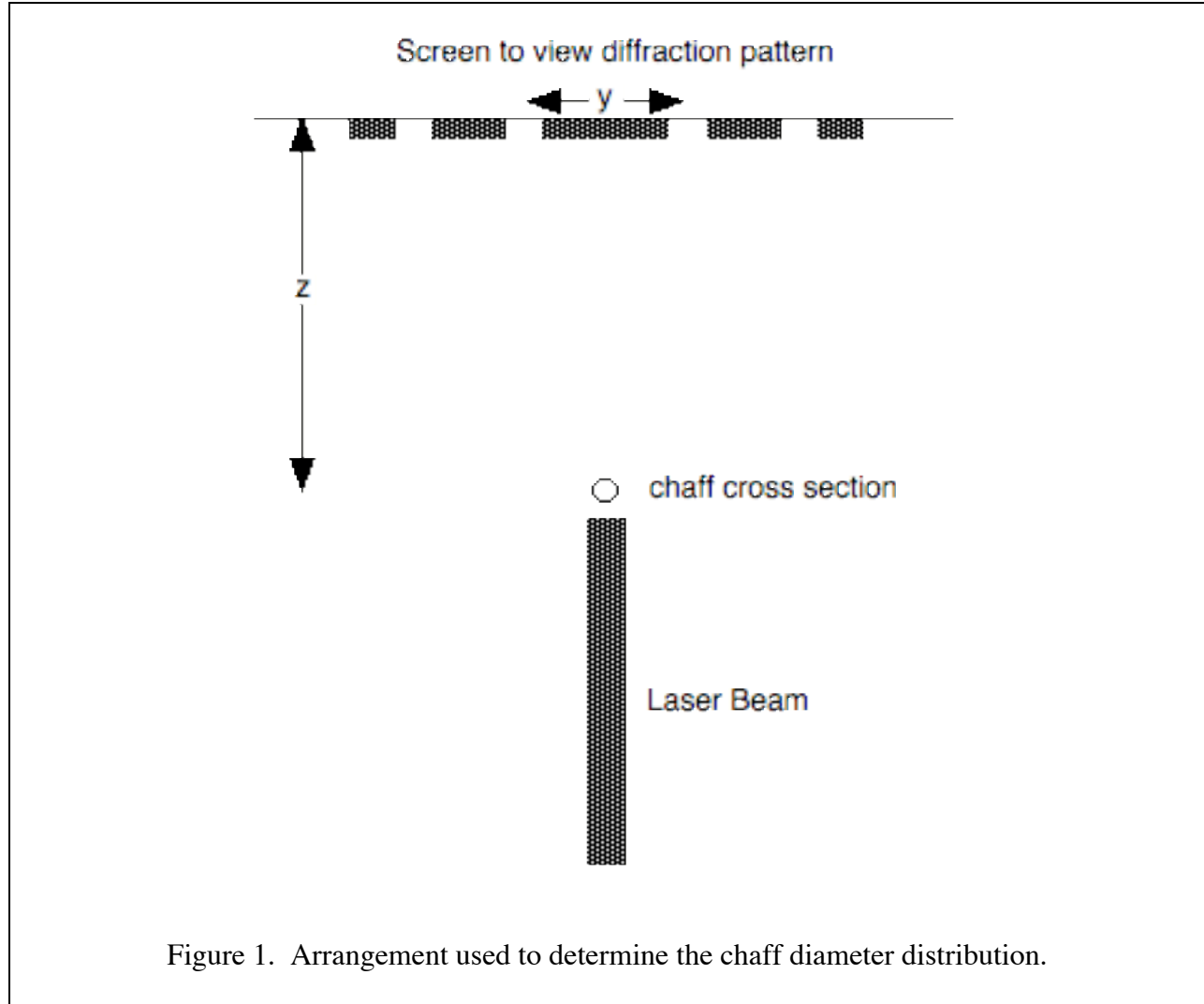
The scenario is as follows. Determine the chaff physical properties including length, average diameter, mass, and density. Estimate the chaff fall speed using available theory as an aid in designing fall tower for measurement of the same. After the fall speed measurements, obtain an equivalent settling velocity, and evaluate the efficacy of the theory. The fall speed work can be used to estimate the time for chaff to fall from the release point in the atmosphere to the ground, as well as to estimate the touch down location. Finally, compute the radar cross section from the measured chaff dimensions and theory. The radar cross section can then be used to invert the NEXRAD radar data to obtain chaff number concentration in the atmosphere from the dBZ_c values.

Measurement of Chaff Diameter Distribution by Laser Diffraction

Figure 1 shows the arrangement used to measure chaff diameter. The basic principle for measurement of the chaff diameter, D , is laser diffraction. Laser light from a 632.8 nm HeNe source is diffracted by the chaff, and the diffraction pattern is observed on a screen. Distances are z and y , the screen-chaff distance and the distance between nulls of the diffraction pattern, respectively. The diffraction pattern associated with a chaff cross section is that of a long rectangular obstacle, and is given by a well-known relation. From diffraction theory, the chaff diameter, D , can be obtained from use of the relation

$$D = \frac{2z\lambda}{y}, \quad (1)$$

where λ is the laser wavelength. The advantage of using laser diffraction to measure D is that distances z and y can be measured quite accurately when the distance from the screen is made large. Typical numbers are $z=132.75''$, $y=6.0''$, and $D=28 \mu\text{m}$.



A total of 103 chaff were taped vertically on a cardboard box with slits in it to allow for laser beam passage. This number provided an adequate estimate of the diameter distribution function, shown in Fig. 2. The observed diffraction pattern was used to calculate the chaff diameter. In some chaff (about 1 in 20), the diameter varied significantly with along the length, though by rotating chaff while viewing the diffraction pattern, it was noted that the chaff cross section appears to be close to uniformly circular. A normal distribution function provided a good fit to the measured diameter histogram. The chaff diameter distribution function is given

by

$$N(D) = N_0 \frac{\exp\left[-(D - \langle D \rangle)^2 / 2\sigma^2\right]}{\sigma\sqrt{2\pi}}, \quad (2)$$

$\langle D \rangle = 28.42 \mu\text{m}, \quad \sigma = 3.30 \mu\text{m}, \quad N_0 = \# \text{ Chaff per Unit Volume}$

where $\langle D \rangle$ is the mean diameter, σ is the standard deviation, N_0 is the total number of chaff per unit volume, and $N(D)dD$ is the number of chaff in the diameter range dD around D per volume.

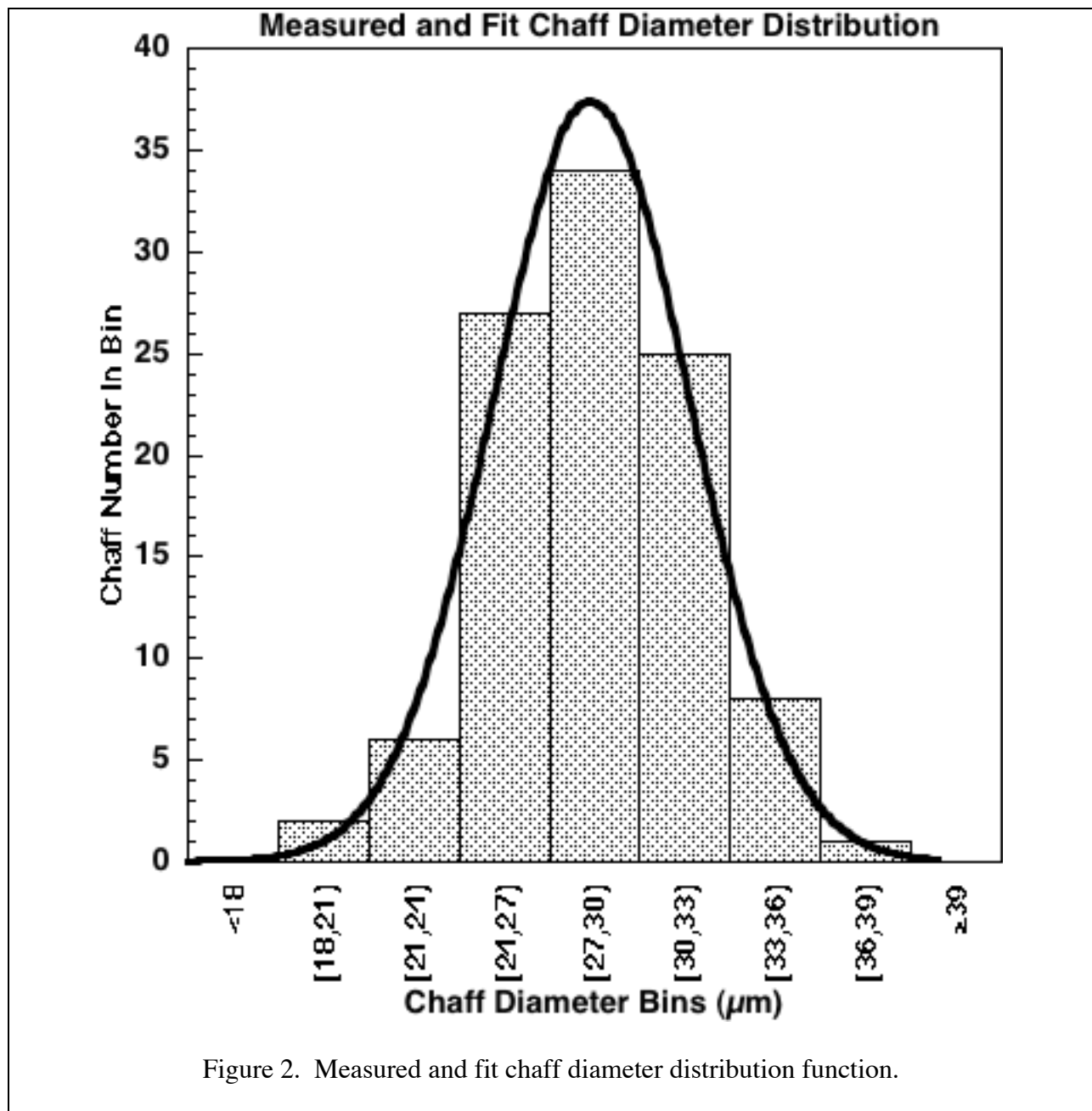
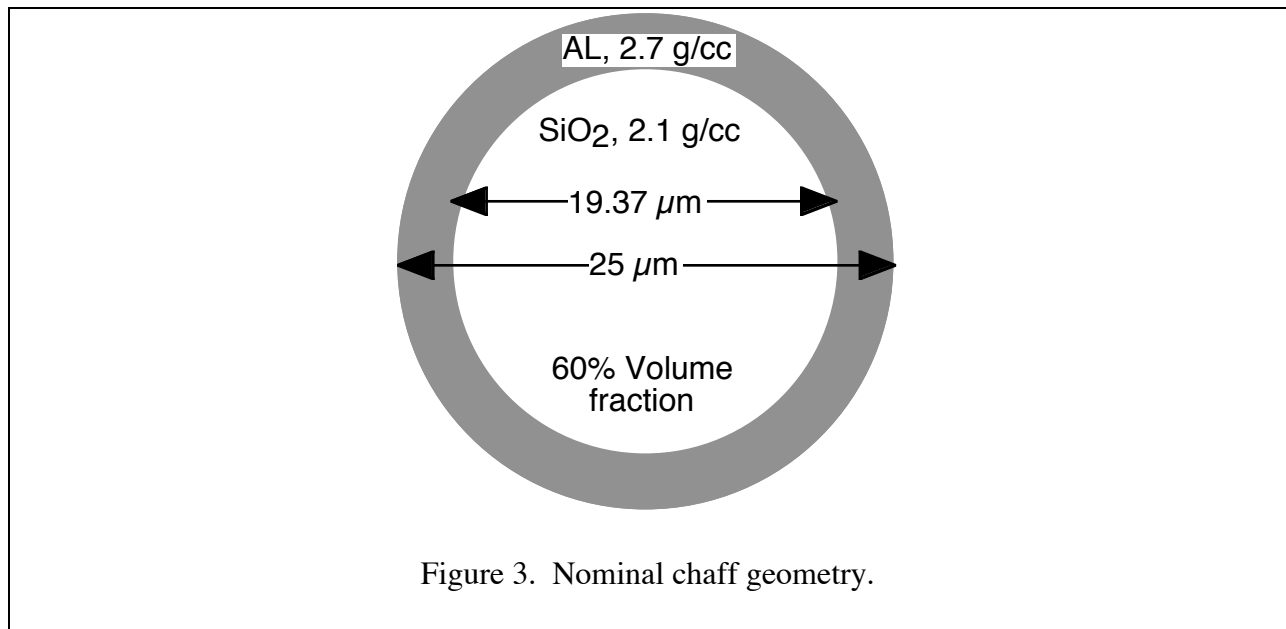


Figure 2. Measured and fit chaff diameter distribution function.

Chaff Mass and Density

The nominal chaff geometry, shown in Fig. 3, consists of an inner core of SiO₂ (amorphous glass) that is 60% of the chaff volume of density 2.1 g/cc, and an outer core of aluminum with density 2.7 g/cc.



Considering the spread of chaff diameters shown in Fig. 2, one possible conclusion is that the outer aluminum layer has a variable thickness. Under this hypothesis, chaff would have a variable density, depending on the aluminum content, as shown in Fig. 4. The density of the nominal chaff shown in Fig. 3 is

$$\rho_{\text{chaff}} = 2.34 \text{ g cc}^{-1}, \quad (3)$$

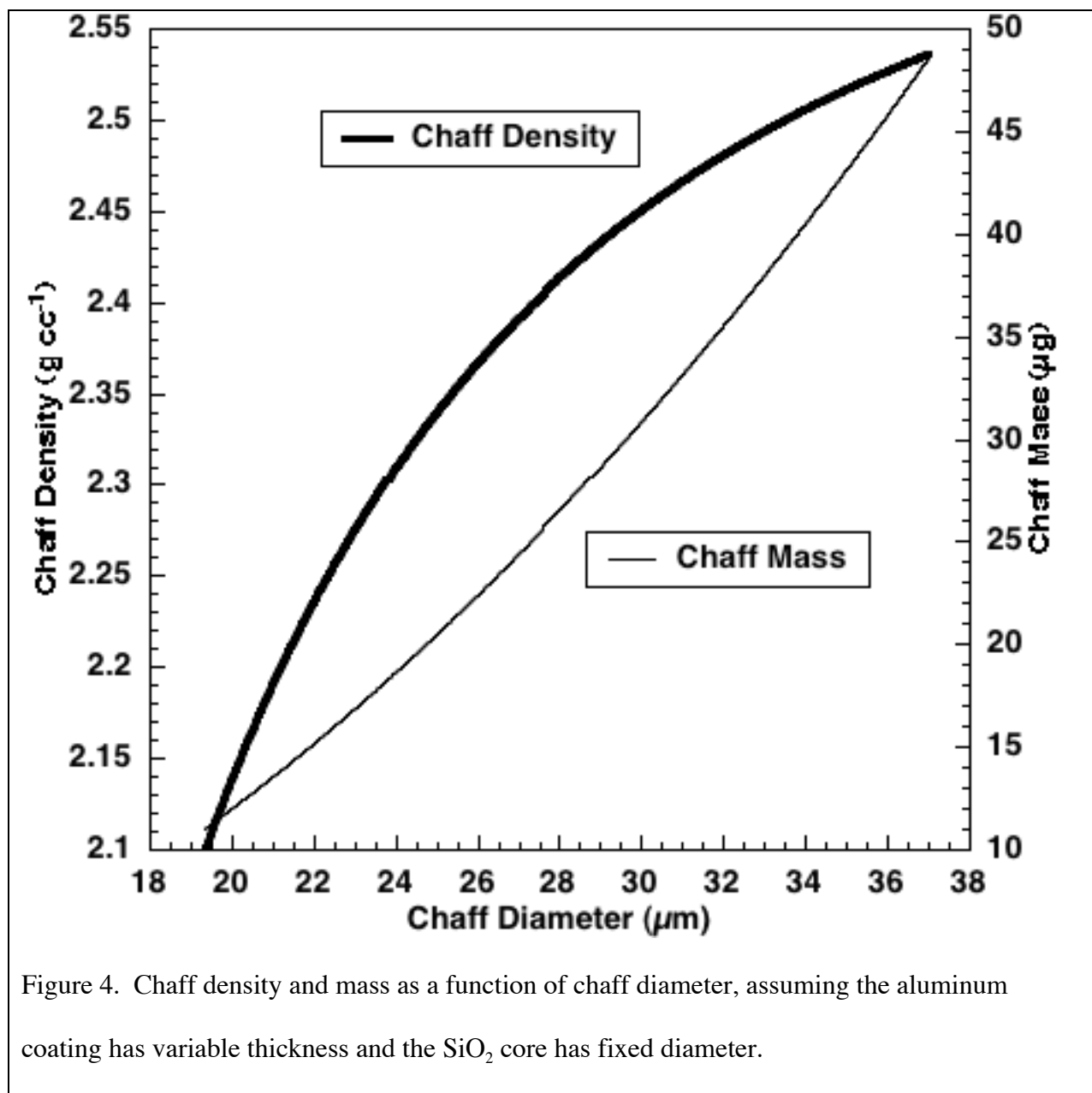
whereas the expression for chaff as a function of diameter, (used to obtain Fig. 4) is

$$\rho(D) = \frac{\rho_{\text{chaff}} 25^2 + \rho_{\text{AL}} (D^2 - 25^2)}{D^2}, \quad D \geq 19.37 \mu\text{m}, \quad \rho_{\text{AL}} = 2.7 \text{ g cc}^{-1}. \quad (4)$$

The chaff diameter, D , enters Eq. (4) in μm units.

Chaff mass was measured by placing approximately 100 particles on the scale, recording the mass, and then removing the particles one at a time to perform an accurate count of their

number. Chaff were sampled from each section of the tube for representativeness. The precision and accuracy of the scale used to measure mass was ± 0.0001 g. Table 1 shows the measured mass, and the number of chaff particles per container, 5.1 million. A chaff diameter, $D_m=28.51$ μm , gives the average mass of 27.5 μg .



measured mass (g)	number of particles	level	Length (cm) (est)		particle mass (microgram)
0.0023	86	1	1.78		26.74
0.0026	83	1	1.78		31.33
0.0031	100	2	1.78		31.00
0.0027	84	2	1.78		32.14
0.003	104	3	1.78		28.85
0.0046	155	3	1.78		29.68
0.0033	122	4	1.78		27.05
0.0024	96	4	1.78		25.00
0.0029	109	5	1.78		26.61
0.003	112	5	1.78		26.79
0.0039	175	6	1.78		22.29
0.0034	151	6	1.78		22.52
				Chaff Mass Average (microgram)	27.50
				Standard Deviation (microgram)	3.39
				Empty chaff container mass (g)	38.5550
				Filled Chaff Container Mass (g)	178.6663
				Number of Chaff in a Container	5,100,000

Table 1. Measured chaff mass and number of chaff in a container.

Chaff Fall Speed

Fall Speed Theory

The theoretical formulation of chaff fall speed will first be presented to gain insight on the requirements for a fall tower used to measure fall speed. Then results of the measurements will be presented.

The equation of motion for a chaff particle is

$$m \frac{dW}{dt} = mg - \frac{\rho_{air} A C_D W^2}{2} \quad , \quad (5)$$

where m is the chaff mass, W is the fall speed, $g = 980 \text{ cm sec}^{-2}$ is the acceleration provided by gravity, ρ_{air} is the air density, A is the chaff cross sectional area, and C_D is the chaff drag coefficient (Juisto and Eadie 1963; Malcolm and Raupach 1991). The drag coefficient for chaff is taken to be that of a horizontally oriented infinite cylinder, and is given by

$$C_D = 10.5 R^{-0.63} \quad (0.5 \leq R \leq 10). \quad (6)$$

The Reynolds number, R , appearing in Eq. (6) is

$$R = \frac{W_T D \rho_{air}}{\mu}, \quad (7)$$

where W_T is the terminal velocity, D is the chaff diameter, and μ is the dynamic viscosity of air.

The terminal velocity is achieved with the fall velocity, W , in Eq. (5) no longer changes with time so that $dW/dt=0$, and is can be obtained from a combination of Eqs. (5) – (7) as

$$W_T = \frac{[(\pi/21) \rho_{chaff} g]^{0.73} D^{1.19}}{\mu^{0.46} \rho_{air}^{0.27}}, \quad (8)$$

where ρ_{chaff} is the chaff density, obtainable as a function of D from Eq. (4). Air density must be corrected for pressure and temperature using the ideal gas law,

$$P = \rho R T / 0.029 \quad (9)$$

where P is the ambient pressure, T is the absolute temperature, and R is the universal gas constant. Air viscosity as a function of temperature can be obtained from (Pierce 1989).

Calculated fall speed as a function of ambient pressure and temperature are given in Table 2. Note that the Reynolds number can go beyond the range listed in Eq. (6). The power law relationship for drag coefficient in this equation appears to be adequate for Reynolds numbers below 0.5, though more analysis of this issue will be given in the fall speed experiment section. The fall speed increases with altitude (pressure drop) because of the air density

diminishment with altitude. The range of fall speed with height is about 15 cm/sec from the surface to the tropopause.

	Pressure (mb)	Temperature (Kelvin)	Air Density (g/cc)	Dynamic Viscosity (g / cm sec)	Reynolds Number	Fall Speed (cm/sec)
	1013.2	288.1	1.23E-03	1.79E-04	0.43	21.9
RENO	850	296	1.00E-03	1.83E-04	0.36	23.0
	616.6	262.1	8.21E-04	1.66E-04	0.36	25.3
	356.5	236.2	5.26E-04	1.53E-04	0.29	29.7
	193.9	216.6	3.12E-04	1.42E-04	0.22	35.3
	103.5	216.6	1.67E-04	1.42E-04	0.14	41.8
	55.2	216.6	8.89E-05	1.42E-04	0.09	49.6

Table 2. Calculated terminal fall speed as a function of pressure and temperature for a chaff

diameter $D = 28.42 \mu\text{m}$.

To estimate the time and distance a chaff must fall before attaining terminal fall speed, as an aid in the experiment design, Eq. (5) can be numerically integrated to obtain the fall speed as a function of time, $W(t)$. The result is shown in Fig. 5. Figure 5 indicates that the largest chaff will attain its terminal velocity before falling 2 cm, so a fall tower length should be much larger than 2 cm long so that the measured fall time will be for chaff falling at its terminal velocity.

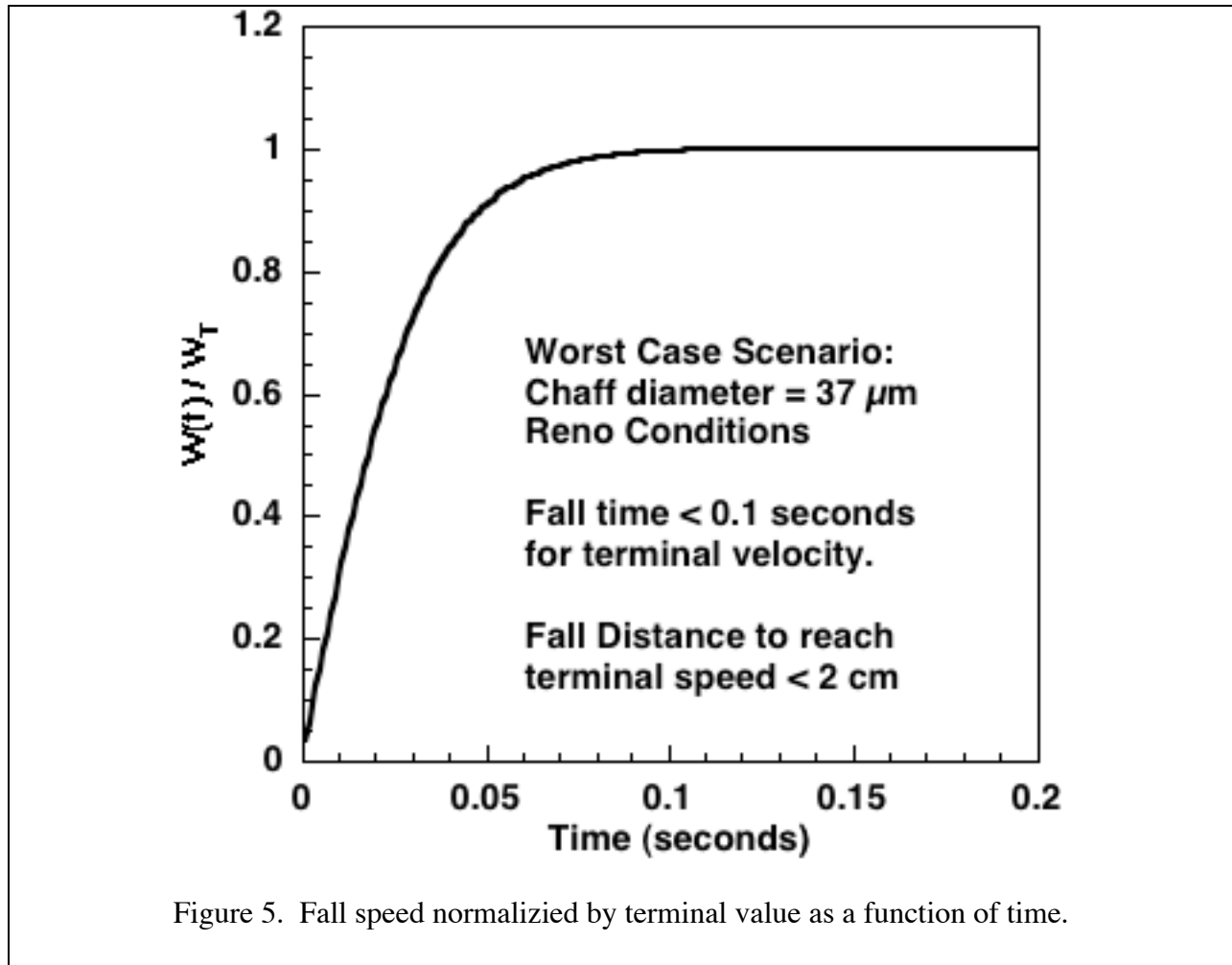
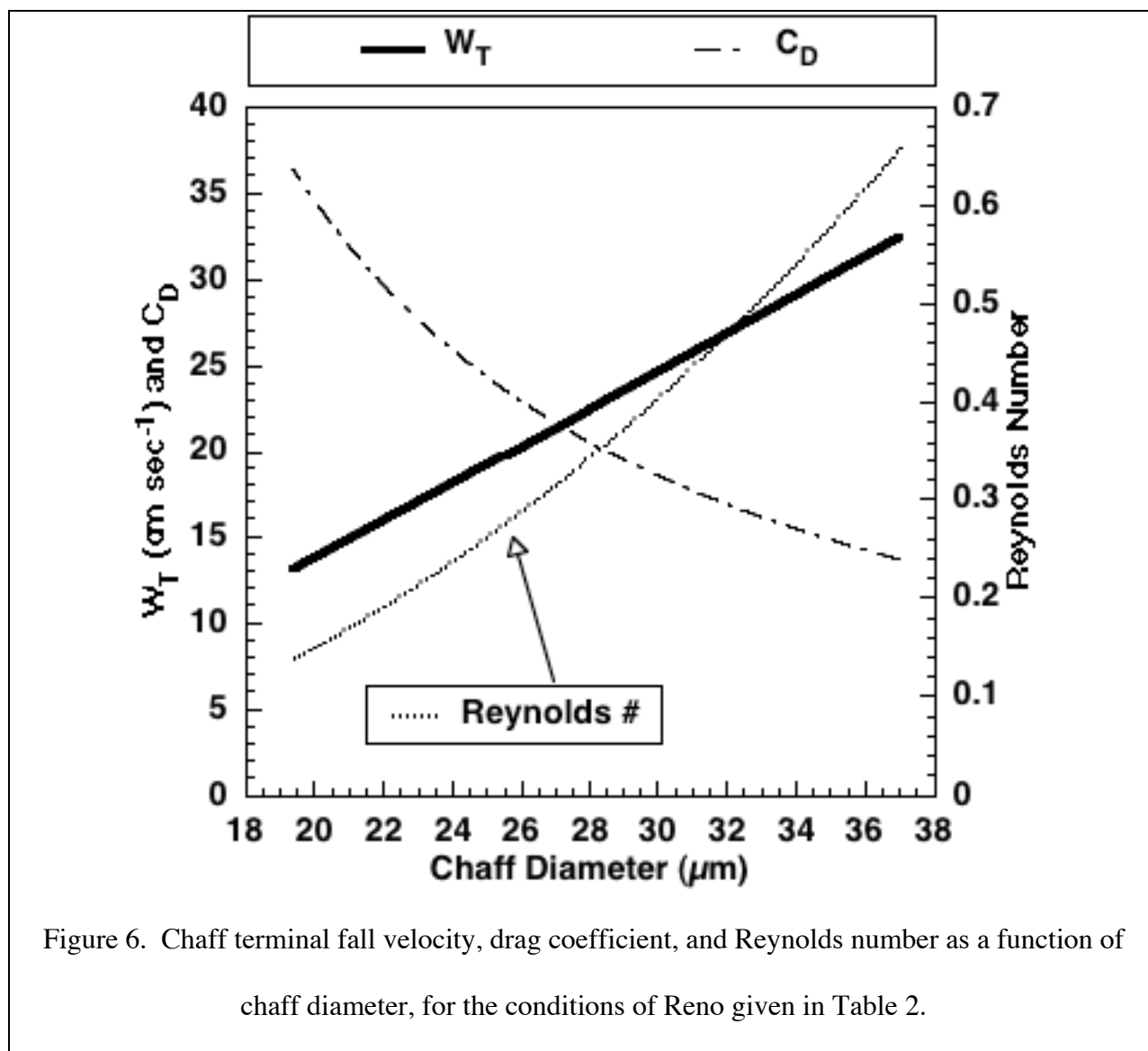


Figure 5. Fall speed normalized by terminal value as a function of time.

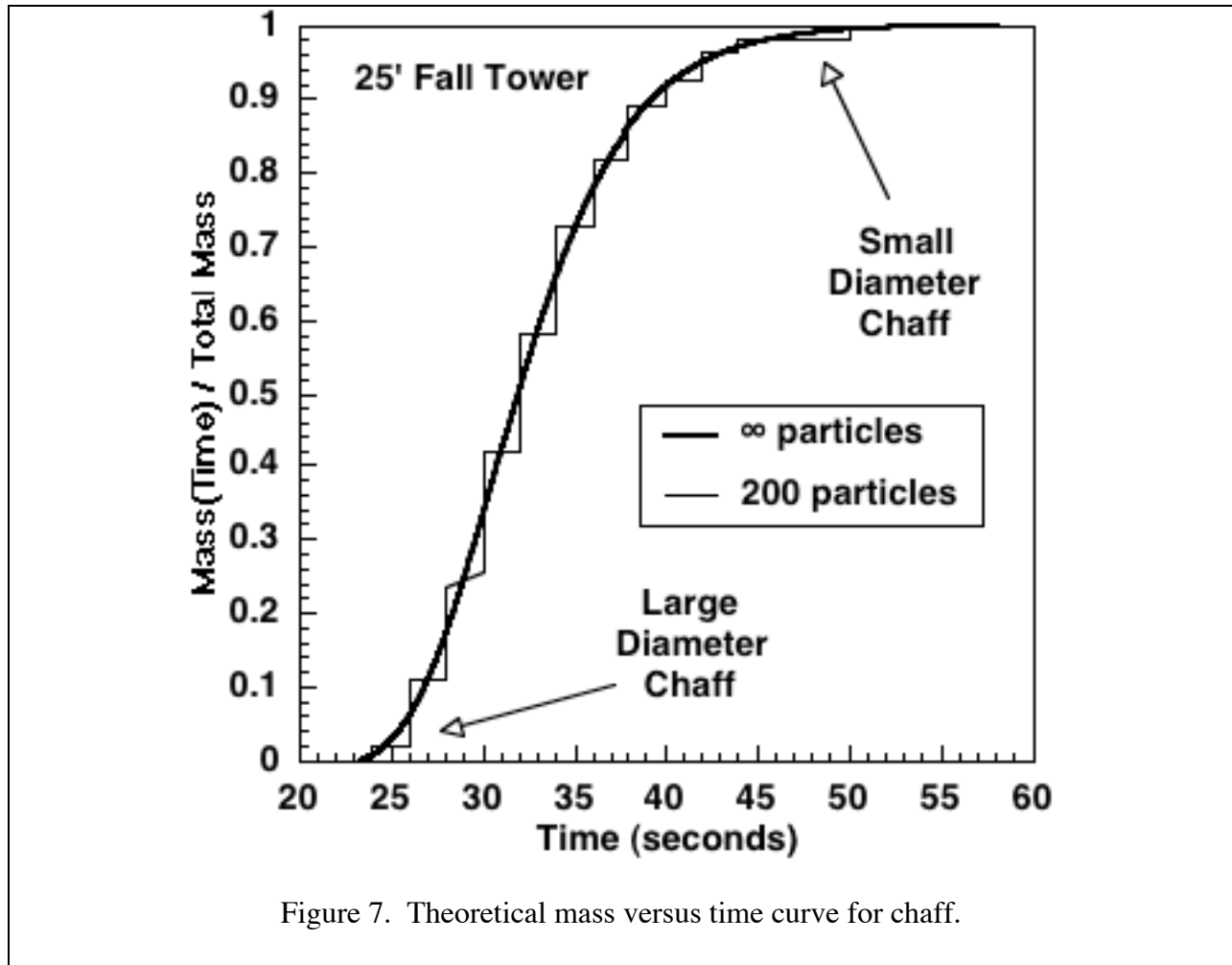
The aerodynamics of chaff are controlled by the chaff diameter because the chaff length (of unbroken chaff) is much larger than the diameter, and the chaff fall in horizontal orientation.

The computed aerodynamics are shown in Fig. 6.



The fall speed is seen to vary between about 13 cm sec^{-1} and 33 cm^{-1} over the diameter range 19 to 37 microns.

The fall tower, to be described below, allows a chaff fall distance of at least 762 cm. A theoretical chaff fall speed experiment is given in Fig. 7.



This curve was computed from the chaff size distribution in Fig. 1, and the chaff aerodynamics, and was made assuming chaff fall the entire distance at the terminal velocity. The largest diameter particles arrive first; smallest arrive last. The thicker curve in Fig. 7 is the ideal mass versus time calculation. The thinner curve takes into account the response time of the mass scale (2 seconds) as well as the scale precision (0.0001 grams) and was obtained assuming 200 particles are used. The discrete form of the mass versus time curve should adequately represent the ideal case.

Chaff Fall Speed Measurements

The fall tower was designed so that chaff could fall 802 cm from release to a fast scale for the mass measurement. The distance chaff must fall to obtain a terminal fall speed is less

than 2 cm, so the error in obtaining fall speed simply as the ratio of fall distance divided by fall speed is less than 1%. Another constraint on the fall tower is that ‘bird-nesting’ should be minimized so that the chaff particles do not clump and fall en-masse. To minimize bird-nesting, approximately 200 chaff particles were released at one time. The precision of the scale used was 0.0001 g per unit, so 4 to 5 chaff particles must accumulate on the scale before the mass changes one unit. The fall height chosen was adequate to resolve the fall time of small and large chaff, as simulated in Fig. 7.

Figure 8 shows images of the fall tower.

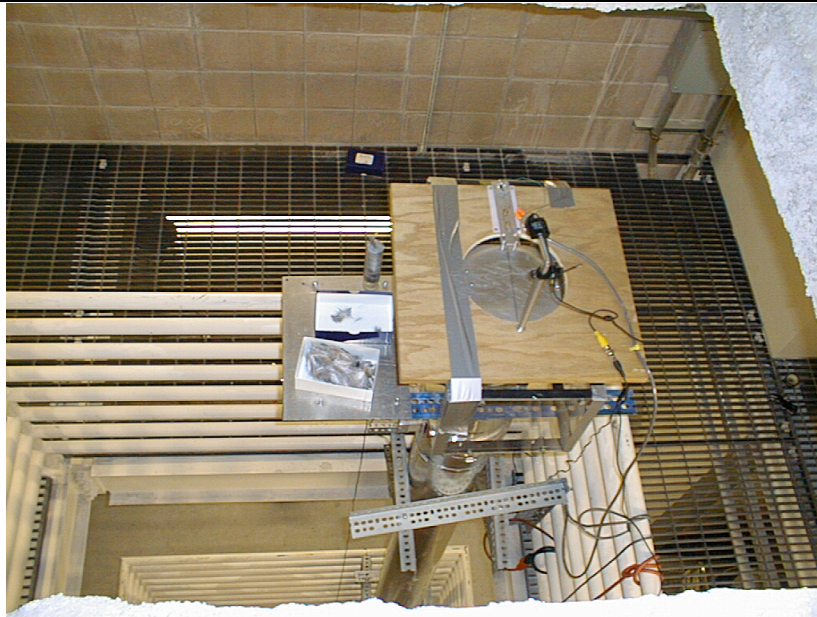


Figure 8a. Photograph of the release mechanism used to deliver chaff to the fall tower. Chaff was placed on the aluminum plates mounted to swing down below the wood platform when the release mechanism was triggered. A miniature black and white video camera, mounted vertically above the aluminum plates, was used to visualize chaff release.

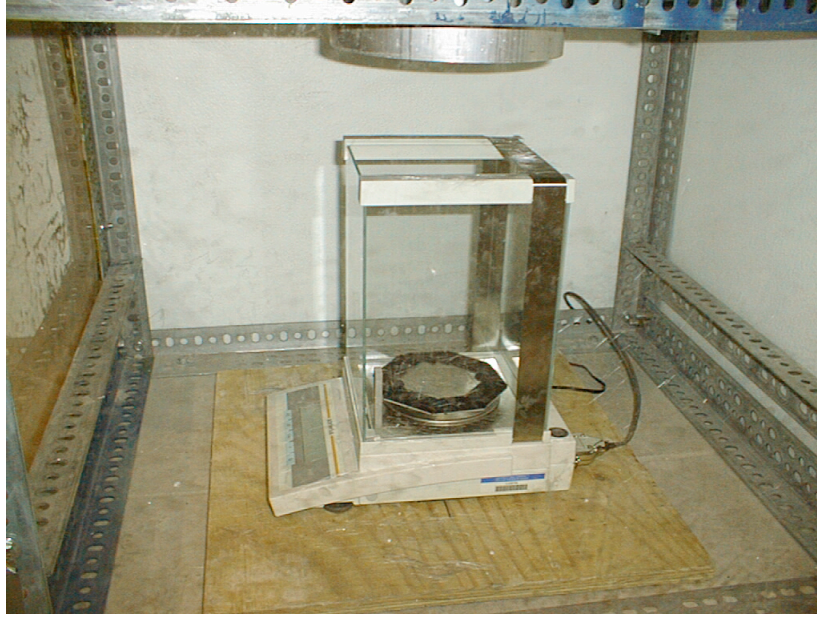
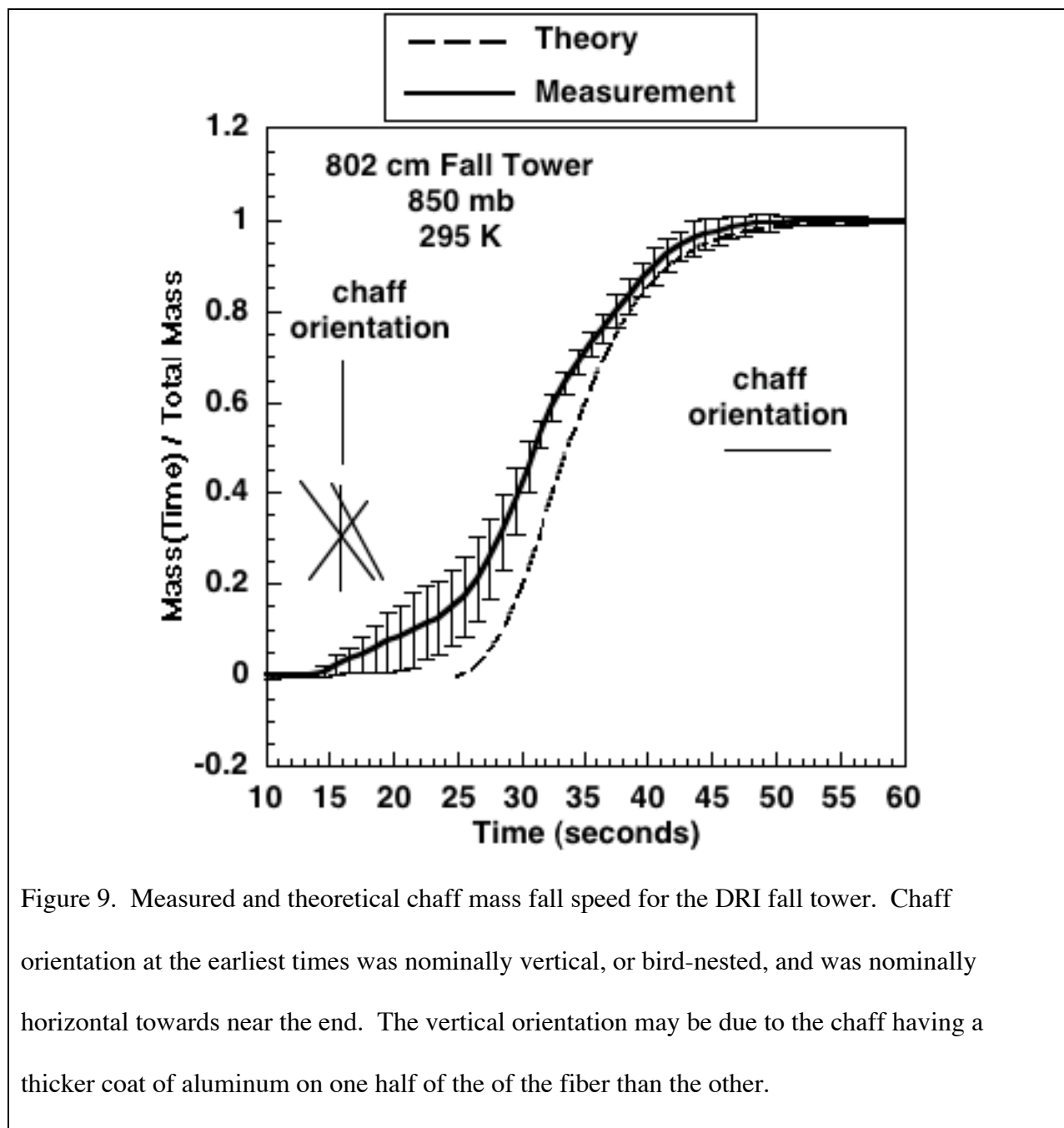


Figure 8b. Image of the scale used to record chaff mass versus time. The fall exit of the fall tower (diameter 8”) is just visible at the top of the photograph. Velcro was applied to the perimeter of the scale plate to reduce chaff fall-off.

Figures 9 shows the average data from the fall tower measurements, along with the theory. The average value was obtained from five measurements. The error bars were computed from the standard deviation of the measurements for each time bin. It is evident that the latest arriving chaff falls at a rate close to the theoretical rate. It was observed with the cameras that the later arriving chaff had nominally horizontal orientation. The theoretical drag law assumes this orientation for the falling cylinders. However, the earliest arriving chaff was predominately vertically oriented as it fell. It is hypothesized that the vertical orientation is due to the chaff having a different thickness of aluminum on one end when compared with the other end, as observed during the laser diffraction measurements of chaff diameter. A second explanation of

t



the anomalously fast chaff fall rate for the early arriving fibers is that some of the chaff inevitably sticks together (bird nests), effectively reducing the surface area of some fibers in the flow, and orienting some fibers in the vertical. Efforts were made to reduce bird nesting, but

approximately 10% of the falling mass was due to bird nested chaff. Such bird nesting of chaff has been observed in operation as well.

Table 3 shows the numerical results of the average chaff fall speed measurements for the data provided in Figure 9. Mass fraction has been set at intervals of 0.1, and total mass is taken to be when 99.5% of the mass has accumulated on the scale.

Table 3

Mass Fraction	Fall Time For 802 cm Tower (sec)	Percentage of Total Fall Time
0.1	21.7	45.5%
0.2	25.9	54.3%
0.3	28.5	59.7%
0.4	29.7	62.3%
0.5	31.7	66.5%
0.6	32.9	69.0%
0.7	34.9	73.2%
0.8	37.7	79.0%
0.9	40.9	85.7%
0.995	47.7	100.0%

Chaff Radar Cross Section

Though chaff is useful as a radar tracer in meteorological studies (Rowland 1976; Reinking and Martner 1996; Murayama, Igarashi et al. 1999), the primary application is in passive jamming of enemy radar (Nathanson, Reilly et al. 1991). In both applications, the chaff user attempts to match the chaff length to approximately $1/2$ of the radar wavelength because standing waves of current excited on the wires give large radar returns. A number of investigations have sought a theoretical understanding of chaff radar returns as a function of wavelength (Van Vleck, Bloch et al. 1944; Van Vleck, Bloch et al. 1947; Puskar 1974; Richmond, Schwab et al. 1974; Garbacz 1978; Guo and Überall 1992; Winchester 1992; Guo and Überall 1993; Pouliguen and Descios 1993). In particular, (Garbacz 1978) has shown that the radar cross section of aluminum-coated fiberglass is very similar to that of a perfectly conducting wire of the same dimensions (in other words, the radar skin depth in the aluminum coating is sufficiently small that the radar hardly detects that a fiberglass core underlies the coating.)

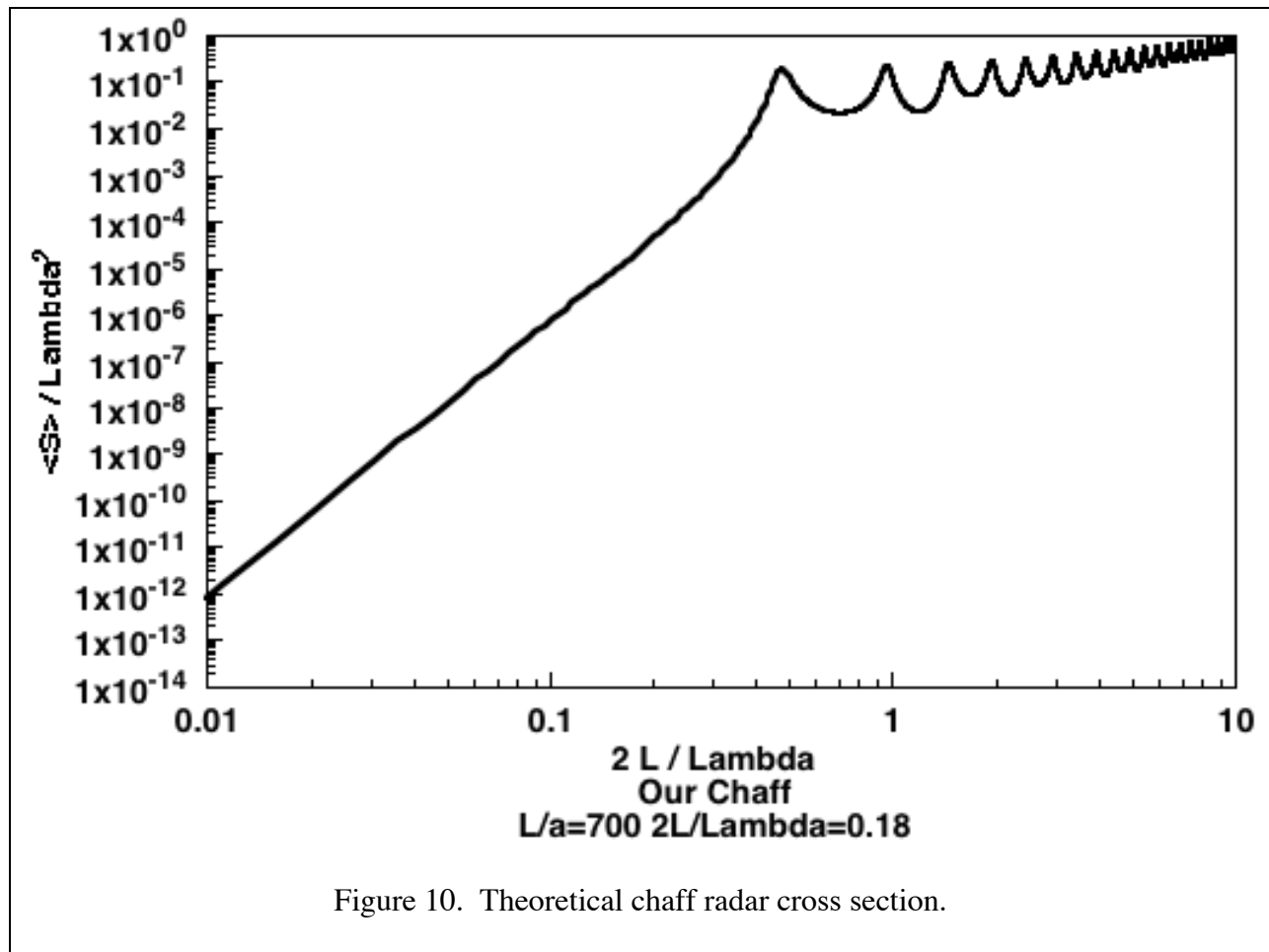
The important parameters for obtaining the chaff radar cross section are the ratios of chaff length:diameter, and chaff length:radar wavelength. It is a deceptively simple problem stated as follows. Obtain the radar cross section of a thin metallic wire. The problem is made more complex if the chaff clump (bird nest), or if the radar cross section is required when the particles are closer than a few radar wavelengths apart, such as immediately after release (Puskar 1974; Nathanson, Reilly et al. 1991). On the whole, individual chaff can be considered well-separated after release, but bird-nesting is likely to agglomerate as much as $1/2$ of the chaff(Nathanson, Reilly et al. 1991). The radar cross section of chaff closer than $1/2$

wavelengths is smaller by a factor of 2 or 3 than it would be if they are well-separated (Puskar 1974).

The chaff radar cross section was computed for a randomly oriented chaff particle based on the analytical formulation developed during WW2 (Van Vleck, Bloch et al. 1944; Van Vleck, Bloch et al. 1947). The computer code based on this theory was checked by successfully repeating the calculations presented in this work, and by noting that at very small ratios of chaff length to radar wavelength, the radar cross section has the correct dependence for Rayleigh scattering (dipole scattering, namely that the cross sections goes as the inverse of the chaff length to the 6th power.) While the equations are too lengthy an opaque to repeat here for the cross sections, the specific approach taken will be described for the interested reader. Referring to (Van Vleck, Bloch et al. 1947) as VV, the angularly dependent radar cross section was computed from EqVV. (37), and was numerically integrated over angle to obtain the average cross section. For chaff of length less than the radar wavelength, the short wire case at the top of pg 291 of VV, and for chaff of length less than 0.15 the radar wavelength, the form above Eq. (39) of VV was used to obtain the proper coefficients for the dipole regime.

The average radar cross section, S , as a function of radar wavelength is shown in Fig. 10. The chaff length is given as $2L$, and the radar wavelength is λ . The series of maxima and minima occurring beyond $2L/\lambda = 0.5$ are due to constructive and destructive interference of standing waves on the wire, and below 0.5, the radar cross section asymptotes to the dipole regime. For the radar wavelength of 10 cm associated with NEXRAD, and for the chaff used by the Navy, the ratio of chaff length to radar wavelength is $2L/\lambda = 0.18$. Note from Fig. 10 that at this value, the radar cross section depends strongly on the chaff length, and in fact goes as the 6th power. One consequence of this dependence is that if small, broken chaff are interspersed

with larger unbroken chaff, it is very likely that the larger chaff will completely dominate the radar return (small chaff are, by comparison, invisible to the radar).



The NEXRAD radar data is processed to be in units relevant to water drops, dBZ_e (Doviak and Zrníc 1993). To make the connection with the radar cross section S , for chaff, consider first the radar reflectivity η as an integral over the product of chaff number ,

$$\eta(D) = \int N(D) S(D) dD, \quad (10)$$

where $N(D)$ (actually N_0 ; see Eq. (2)) is the sought after chaff number concentration. The radar reflectivity can be redefined in relation to the reflectivity factor for water drops

$$\eta = \frac{\pi^5}{\lambda^4} |K_w|^2 Z_e \quad , \quad (11)$$

where λ is the radar wavelength, $K_w = (m^2 - 1)/(m^2 + 2)$ is obtained from the complex refractive index at the radar wavelength, m , of water, and Z_e is the equivalent reflectivity factor. For the NEXRAD radar, $|K_w|^2 = 0.93$. The quantity actually reported by NEXRAD is

$$dBZ_e = 10 \text{ LOG}_{10}(Z_e) \quad . \quad (12)$$

Inverting Eqs. (10) – (12), the chaff number concentration is related to radar data by

$$N_0 \text{ (chaff/cubic kilometer)} = 13400 * 10^{(dBZ_e/10)} \quad (13)$$

where \wedge is to the ‘power of’ operator. For example, with $dBZ_e = 25$, the $N_0 = 4.24\text{E}+06$ chaff per cubic km. Given that there are approximately 5.1×10^6 chaff per tube, the number concentration can be rephrased as the number of delivery tubes per cubic km = 0.83, so that the radar volume for 1 delivery tube dispersed in the atmosphere is = 1.20 cubic kilometers.

Chaff Radar Cross Section for Inhomogeneous Chaff Delivery Tubes

Equation (13) is relevant only to the R144 chaff. Other chaff can be delivered in tubes containing sections of various lengths, with the objective of blocking a variety of radar wavelengths as shown schematically in Fig. 11.



Figure 11. Schematic view of an inhomogeneous chaff delivery tube having 1 section of longest chaff, and 2 sections each of progressively shorter chaff.

The basic scenario is illustrated in Fig. 12. Radar is used for detection of airplanes, or for radar meteorology of the atmosphere. An airplane blows out one or more chaff tubes for training purpose, with the ultimate goal in mind of confusing enemy radar and in preventing a successful missile strike. Once emitted from the airplane, the chaff follows the prevailing winds, and falls to the Earth under gravity, as modified by any updrafts or downdrafts that might happen to be present. Usually the horizontal winds (parallel to the Earth's surface) are much greater than the vertical winds, so chaff released at altitude can be carried many miles downwind before it is deposited on the ground.

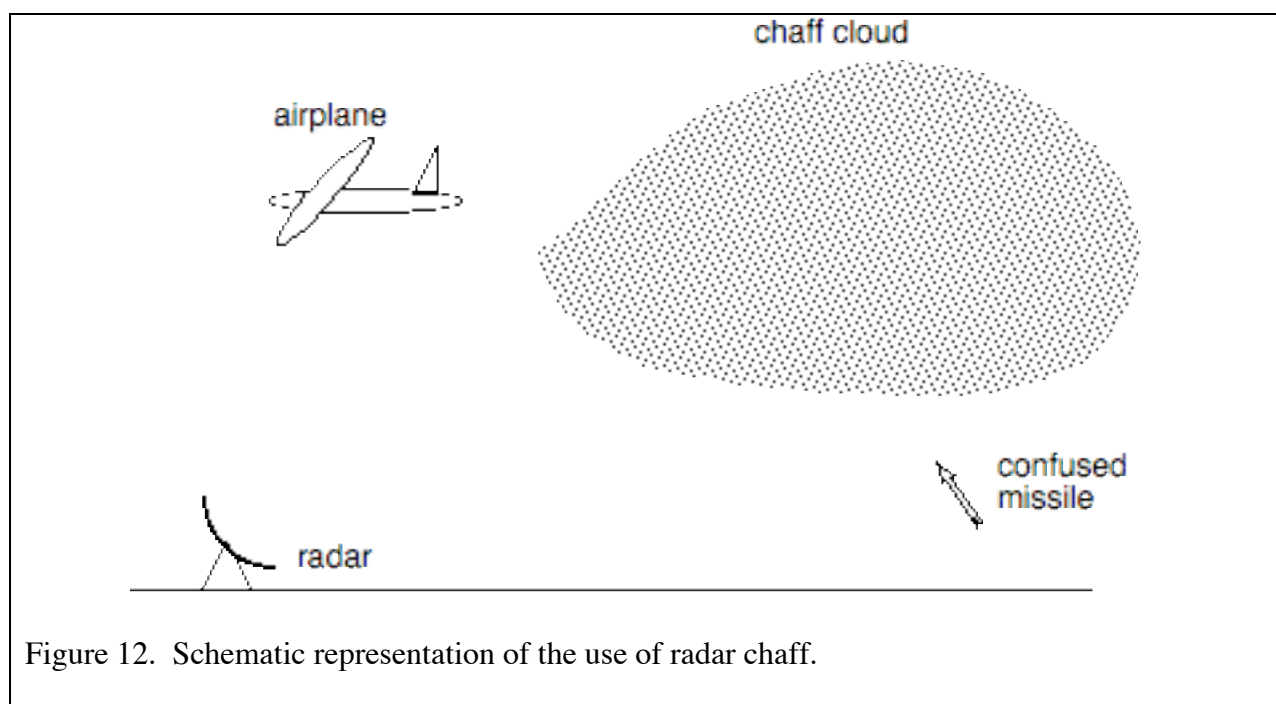


Figure 12. Schematic representation of the use of radar chaff.

It is clear from the fall speed measurements, and comparison with theory, that chaff having different lengths will still have the same fall velocity, because the fall speed is dependent on the chaff radius, not its length. On the other hand, the radar cross section calculation shown in Figure 10 indicates that chaff length is extremely important for determining its radar cross section. The basic physics is quite simple, if the chaff length is an integer number of $1/2$ radar wavelengths, the radar can set up standing waves of current on the chaff (wire) that radiate

prodigiously. To confuse missiles, it is best to use a chaff that is of the will have a huge radar cross section. On the other hand, if the chaff length is much shorter than the radar wavelength, as on the left side of the graph in Figure 10, the radar cross section will be much smaller than it is at resonance (but still much larger than the radar cross section of many hydrometeors in the atmosphere such as water drops, ice crystals, etc.). The radar cross section can vary dramatically with chaff length. So if a inhomogeneous chaff tube is used, as illustrated schematically in Fig. 11, and a variety of chaff lengths are present, the radar is going to respond strongest to the longest chaff. It is possible that the relative signal of long and short chaff in a tube is such that the radar cross section of the long chaff is so much greater than that of the short chaff that the short chaff can not be seen. The long chaff essentially masks the short chaff.

The single chaff length theory developed in the previous section must now be expanded to include the effect of chaff tubes having an assortment of chaff lengths in it. To make the connection with the radar cross section S , for chaff of varying length, consider first the radar reflectivity η ,

$$\eta = m N_s \sum_{i=1}^{\#ChaffLengths} \left\{ n_i \int \frac{N(D)}{N_0} S_i(D, L_i) dD \right\}, \quad (14)$$

where $N(D)/N_0$; (see Eq. (2)) is the normalized chaff diameter distribution function, m is the sought after number of chaff tubes released per unit volume, N_s is the number of chaff in one segment of the chaff tube (7.3×10^5), n_i is the number of sections in the chaff tube where the section length is $2L_i$, and the radar cross section is of course a function of chaff diameter and length and radar wavelength. For example, in the R144 chaff, all 7 segments have the same length, so the summation index ranges only to unity, and $n_i = 7$.

In a manner equivalent to the development of the method for computing single chaff number from the radar return, as given in Eqs. (11) – (13), the chaff number per unit volume can be expressed as

$$m(\text{chaff tubes/cubic kilometer}) = \alpha * 10^{(dBZe/10)} \quad (15)$$

Different types of chaff will have different prefactors, α , so an assortment of chaff tubes have been assumed. Table 2 shows the prefactor to use for various chaff types. The number of chaff per unit volume is determined by multiplying the number of chaff tubes per unit volume in Eq. (15) by the number of chaff in the tubes.

The fractional contribution, f_i , of chaff of a particular length to the total radar cross section can be determined from

$$f_i = \frac{\left\{ n_i \int \frac{N(D)}{N_0} S_i(D, L_i) dD \right\}}{\sum_{i=1}^{\#ChaffLengths} \left\{ n_i \int \frac{N(D)}{N_0} S_i(D, L_i) dD \right\}} \quad (16)$$

The radar weighted chaff number is obtained from

$$N_{radar} = N_s \sum_{i=1}^{\#ChaffLengths} \{ n_i f_i \} \quad (17)$$

By comparison, the number of chaff particles in a tube is given by

$$N_{Total} = N_s \sum_{i=1}^{\#ChaffLengths} \{ n_i \} \quad (18)$$

The ratio N_{radar}/N_{total} is unity for a homogeneous chaff tube containing fibers of all the same length, and is less or equal to unity otherwise. In essence, the NEXRAD radar is most sensitive to the larger fibers, so N_{radar} is a measure of how many chaff fibers can be detected from the radar signal. Even though the radar will not be equally sensitive to all chaff fibers, depending on their

lengths, the total number of fibers in the atmosphere can still be obtained if the type of chaff delivery tube used is specified.

Table 4 contains the description of five commonly used chaff types. These chaff tubes differ only in that they contain chaff fibers of different lengths, as illustrated in Fig. 11. The fall speed measurements and the radar cross section calculation earlier were done with R144 chaff. Note that three types of chaff (R129, R170, and R184) all contain 5.08 cm chaff fibers. These fibers are likely at the first resonance of the NEXRAD radar cross section (the first peak from the left in Fig. 10). All other fibers are shorter, so their radar cross section lies in the monotonically increasing section of the radar cross section in Fig. 10, e.g. the Rayleigh regime.

Table 4

Chaff Designation	# Fibers Per Tube	Fiber Lengths (cm)	# Sections Each Fiber Length
R144	5.1 Million	1.78	7
R129	3.6 Million	1.55, 2.84, 5.08	3, 1, 1
R170	3.6 Million	0.75, 1.78, 2.2, 2.5, 5.08,	1, 1, 1, 1, 1
R184	2.9 Million	1.27, 1.52, 2.54, 5.08	1, 1, 1, 1
R189	2.9 Million	0.99, 1.32, 1.88	2, 1, 1

Table 5 gives the computed prefactor, α , to go from radar cross section in dBZe to the number of chaff tubes per cubic km (see Eq. (15)). It also gives the contribution of each set of fiber lengths to the total radar return. In all cases where the 5.08 cm fibers are in the tubes, essentially 100% of the radar return comes from these fibers; these long fibers in a way mask or hide the shorter fibers from the radar.

Table 5

Chaff Designation	Prefactor α	Fiber Lengths (cm)	Radar Fraction Each Fiber Length
R144	2.627E-3	1.78	100
R129	3.902E-6	1.55, 2.84, 5.08	0, 0, 100
R170	3.908E-6	0.75, 1.78, 2.2, 2.5, 5.08,	0, 0, 0, 0, 100
R184	3.910E-6	1.27, 1.52, 2.54, 5.08	0, 0, 0, 100
R189	1.134E-2	0.99, 1.32, 1.88	5, 12, 83

Table 6 contains further quantities computed about the radar return of the chaff. For each chaff, the fraction of fibers observable with the NEXRAD 10 cm radar (obtained from the ratio of Eqs. (17) and (18)) is given in the second column. The longer chaff ‘hide’ the shorter ones, so only a fraction are observable by radar. The final column of Table 6 gives an example of the inversion of the NEXRAD radar return given in dBZe to obtain the number of chaff tubes per cubic kilometer for a signal of 55 dBZe. Note that the tubes containing 5.08 cm long fibers correspond to a reasonable 1-2 chaff tubes per cubic km; however, the tubes containing only short fibers would require on the order of 1000 tubes to produce a signal level of 55 dBZe. It is not likely at all that 1000 tubes of chaff are blown all at once! So this is a guide to use in evaluating the reasonableness of the inversion.

Finally, Fig. 13 shows the computed inversion curves for various chaff types. Note that three different tubes have the same inversion, owing to the dominant influence of the long fibers. Loosely, small radar cross sections are likely due to either the R189 or R144 chaff, and high returns are likely due to any of the R129, R170, or R184 chaff types.

Table 6

Chaff Designation	Fiber Percentage Observable By NEXRAD radar	#Chaff Delivery Tubes / cubic km for a 55 dBZe NEXRAD radar signal
R144	100%	831
R129	20%	1.23
R170	20%	1.23
R184	25%	1.24
R189	26%	3586

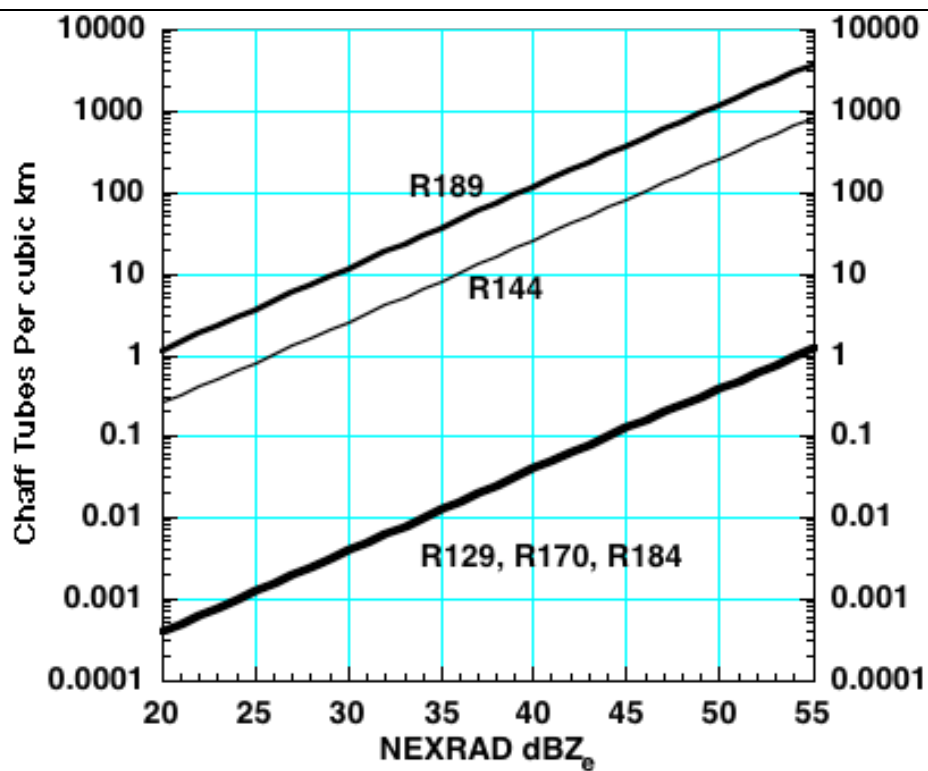


Figure 13. Inversion of the NEXRAD radar signals to obtain the number of chaff tubes per cubic km.

REFERENCES

Doviak, R. J. and D. S. Zrnic (1993). Doppler Radar and Weather Observations. San Diego, CA, Academic Press.

Garbacz, R. J. (1978). Chaff Radar Cross Section Studies and Calculations. Columbus, Ohio, Ohio State University: 36.

Guo, Y. and H. Überall (1992). "Bistatic radar scattering by a chaff cloud." IEEE Transactions on Antennas and Propagation **40**: 837-841.

Guo, Y. and H. Überall (1993). "Radar depolarization in the ground-based system due to chaff." Journal of Electromagnetic Waves and Applications **7**: 197-213.

Juisto, J. E. and W. J. Eadie (1963). "Terminal fall velocity of radar chaff." Journal of Geophysical Research **68**: 2858-2861.

Malcolm, L. P. and M. R. Raupach (1991). "Measurements in an air settling tube of the terminal velocity distribution of soil material." Journal of Geophysical Research **96**: 15275-15286.

Murayama, Y., K. Igarashi, et al. (1999). "Wind observations in the MLT region over Southern Japan, by using foil chaff technique, Yamagawa MF radar and the MU radar." Adv. Space Res. **24**: 575-578.

Nathanson, F. E., J. P. Reilly, et al. (1991). Radar Design Principles. Mendham, NJ, Scitech.

Pierce, A. D. (1989). Acoustics: An Introduction to Its Physical Principles and Applications.

Woodbury, New York, Acoustical Society of America.

Pouliguen, P. and L. Descios (1993). "Model of the polarimetric behavior of chaff media."

Microwave and Optical Technology Letters **6**: 214-218.

Puskar, R. J. (1974). "Radar reflector studies." NAECON 74 **74**: 177-183.

Reinking, R. F. and B. E. Martner (1996). "Feeder-Cell ingestion of seeding aerosol from cloud-base determined by tracking radar chaff." Journal of Applied Meteorology **35**: 1402-1415.

Richmond, J. H., L. M. Schwab, et al. (1974). "Tumble-average radar backscatter of some thin-wire chaff elements." IEEE Transactions on Antennas and Propagation **22**: 124-126.

Rowland, J. R. (1976). "Clear air convective behavior revealed by radar chaff." Journal of Applied Meteorology **15**: 521-526.

Van Vleck, J. H., F. Bloch, et al. (1944). Theory of the radar response of chaff, REPORT 411-103, Harvard University Radio Research Laboratory: 51.

Van Vleck, J. H., F. Bloch, et al. (1947). "Theory of radar reflection from wires or thin metallic strips." journal of Applied Physics **18**: 274-294.

Winchester, T. A. (1992). "Pulsed radar return from a chaff cloud." IEEE Proceedings F **139**: 315-320.